RSC Advances

PAPER

View Article Online
View Journal | View Issue

Cite this: *RSC Adv.*, 2018, **8**, 24780

Microwave absorption properties of lightweight and flexible carbon fiber/magnetic particle composites

Wei Ye, *[ab] Wei Li,[ab] Qilong Sun,[ab] Jin Yu[ab] and Qiang Gao[a]

Hybridized-carbon-based materials with magnetic metals and oxides have attracted much attention because of their enhanced electromagnetic wave loss. In this study, magnetic particles were coated on the surface of carbon fibers by carbonizing in a nitrogen atmosphere. The morphology, structure, thermolysis, and wave-absorption performance of the carbon fiber/magnetic particle composite were determined. Results show that the *in situ*-formed magnetic particles (such as Fe_3O_4, $NiFe_2O_4$, $CoFe_2O_4$, and Ni_3Fe) are uniformly dispersed along the carbon-based fibers, which exhibit different wave absorption. The absorption of the carbon fiber/magnetic particle composite can be controlled by adjusting the species and concentration of the magnetic particle coating, which provides a new and effective way of endowing the magnetic-particle-coated carbon fibers with good microwave absorption properties.

Received 13th June 2018
Accepted 2nd July 2018

DOI: 10.1039/c8ra05065a

rsc.li/rsc-advances

Introduction

Radar-absorbing materials (RAMs) are used to cover the surface of targets in order to reduce target detection by radar, *i.e.*, to reduce the radar signature (radar echo). In addition, RAMs can reduce the impact of electromagnetic pollution. Therefore, RAMs are of great importance, both in civilian and military fields, and have attracted great attention globally. To date, many studies have been carried out on new high-performance electromagnetic absorbers with light materials, wide absorption bands, and low cost. Carbon materials, such as carbon fibers (CFs), reduced graphene oxide (RGO), and carbon nanotubes (CNTs), which are a typical subject of research, have proved effective as RAMs.[1–5] Carbon fibers, which are suitable substrate materials owing to their low density, high strength, and excellent electrical properties, are used to prepare carbon fiber nonwovens and other absorbing materials.[1,6] Carbon fibers are also combined with other polymers, such as polyaniline and epoxy resin, to obtain absorbing materials in order to improve their microwave-absorbing capacity.[7,8]

However, carbon materials are a type of electromagnetic-wave-absorbing materials that exhibit dielectric loss. When a pure carbonaceous material is used, the absorbing property of the material is[9,10] affected by its low magnetic loss and high reflection coefficient. To mitigate this defect, researchers have used electroplating, co-precipitation, or coating on the surface of carbon materials to load magnetic particles such as carbonyl-iron, Fe_3O_4, Ni, and Fe–Co in order to enhance the absorption properties of the material.[11–14] It is worth noting that magnetic materials based on Fe, Co, and Ni with better soft magnetic properties are coated on CFs, RGO, and CNTs, and other carbon materials, which can effectively combine their advantages, reduce the disadvantages of dielectric loss and magnetic loss in these materials, thus providing a lightweight and wide-absorption-band-absorbing composite material.[15–18]

However, electroplating, chemical plating, and reduction are usually adopted to prepare magnetic coatings on carbon fibers. The drawbacks of these methods are time consumption, low yield, and uncertain quality, and effect on the coat of the internal fiber.

In this study, for the first time, core (CFs)–shell (magnetic particle) hybrids with light and soft were prepared *via* a simple, low-pollution, high-temperature one-step molding process. The magnetic and microwave absorption properties of the CF/magnetic particle composites were then investigated.

Experimental

Preparation of CF/magnetic particle composite

The preparation process is schematically illustrated in Fig. 1. Polyacrylonitrile (PAN)-based pre-oxidative felt (fiber diameter of 1.5 dtex) was obtained from Nantong Sen Carbon Fiber Co., Ltd. Prior to impregnation, the felts were cleaned at 60 °C for 30 min in ethanol. A metal salt solution (different proportions of $FeCl_3$, $CoSO_4 \cdot 7H_2O$, and $NiSO_4 \cdot 6H_2O$) was employed for the impregnation of PAN-based pre-oxidative felts. After drying, the PAN-based pre-oxidative fibers containing metal salts were heat-

[a]National & Local Joint Engineering Research Center of Technical Fiber Composites for Safety and Protection, Nantong University, Nantong 226019, P. R. China
[b]College of Textiles and Clothing, Nantong University, Nantong 226019, P. R. China. E-mail: 247173958@qq.com

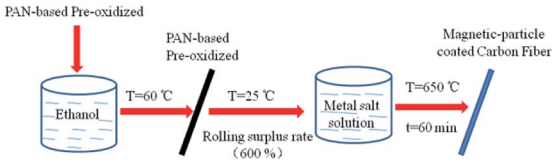

Fig. 1 Preparation process for magnetic-particle-coated carbon fiber.

treated at 650 °C for 60 min in N_2. CF/FeCoNi, CF/FeCo, CF/FeNi, and CF/CoNi were prepared according to different ratios of the impregnating solution [n(Fe) : n(Co) : n(Ni)], of 2 : 2 : 1, 2 : 2 : 0, 2 : 0 : 1, and 0 : 2 : 1, and the concentration of the total metal ions was 0.625 mol L^{-1}. CF/FeCoNi was prepared under different concentrations (0.625 × 0 mol L^{-1}, 0.625 × 0.5 mol L^{-1}, 0.625 × 1 mol L^{-1}, 0.625 × 1.5 mol L^{-1}, 0.625 × 2 mol L^{-1}, and 0.625 × 2.5 mol L^{-1}).

Characterization

Phase structure analysis of the prepared CF/magnetic particle was performed using X-ray diffraction (XRD, Rigaku D/max-2500PC, with CuK_α). A scanning electron microscopy (SEM, Scios DualBeam) system equipped with energy dispersive spectroscopy (EDS) apparatus was used for morphology observation and elemental analysis, respectively. The formation mechanism was analyzed using thermogravimetry/differential scanning calorimetry (TG/DSC, Netzsch 214 Polyma) at a heating rate of 5 °C min^{-1} from 30 to 800 °C in argon atmosphere. The reflection coefficient (RC) of the CF/magnetic particle composite was determined in the frequency ranges of 5.85–8.2 GHz, 8.2–12.4 GHz, 12–18 GHz, and 18–26 GHz by the NRL-arc method. A metal sheet (180 mm × 180 mm) and CF/magnetic particle composite with the same dimensions were successively placed on the sample platform. Two horn antennas were used to send and receive the electromagnetic wave normally with the sheet.

Results and discussion

Phase composition and morphology

The PAN-based pre-oxidized felt after impregnation with metal salts was treated for 60 min at 650 °C in N_2. The interaction between the fiber and metal salt produces complex particles. The XRD patterns of the pure carbon powders (Fig. 2a) show only one extremely broad diffraction peak, which is attributed to the crystallographic (0 0 2) plane of graphite in the turbostratic carbon structure.[19] In the CF/magnetic particle composite, this peak broadens and shifts slightly towards high 2θ. The strong diffraction peaks with a small full-width at half maximum indicate good crystallization of the sample. In Fig. 2a, we can observe CF/FeCoNi contained by Fe_3O_4 (JCPDS 75-1609), $NiFe_2O_4$ (JCPDS 74-2081), $CoFe_2O_4$ (JCPDS 79-1744), Ni_3Fe (JCPDS 88-1715), and other magnetic particles; it also includes (Co, Ni, Fe)$_9S_8$ (JCPDS 30-0444) and other nonmagnetic particles. The magnetic properties of these magnetic particles appearing in the XRD pattern clearly exhibit magnetic loss. In reality, they are also applied to

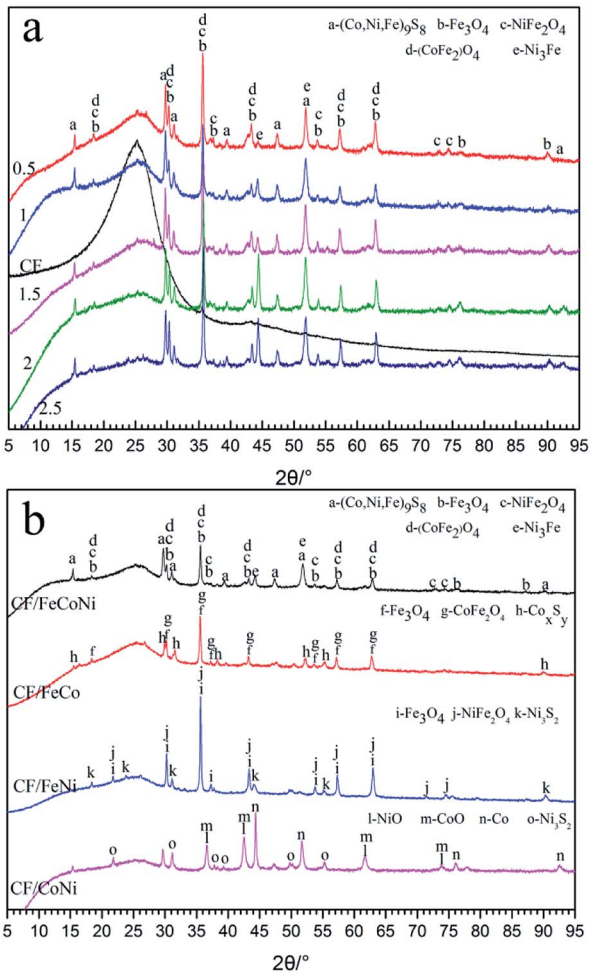

Fig. 2 XRD patterns (a and b) of CF/FeCoNi prepared at 0.5, 1, 1.5, 2, and 2.5 times concentrations; CF/FeCoNi (1 times), CF/FeCo, CF/FeNi, CF/CoNi.

magnetic loss composites.[13,15,17] When we change the concentration of the impregnated solution, the position of the characteristic peak in the XRD diagram does not change; only the Ni_3Fe characteristic peak becomes stronger. Therefore, we can conclude that the level of concentration does not affect the change in the final magnetic particle type. However, when only two types of metal salts are prepared with the impregnation solution, the particles generated are different from CF/FeCoNi, and there are different phases in the same substance. When there are only two types of metal salts in the solution, we find that CF/FeCo is coated by particles such as Fe_3O_4 (JCPDS 75-0499), $CoFe_2O_4$ (JCPDS 22-1086), CoxSy (JCPDS 75-1561, and JCPDS 25-2023); CF/FeNi is coated by particles such as Fe_3O_4 (JCPDS 86-2267), $NiFe_2O_4$ (JCPDS 86-2267), and Ni_3S_2 (JCPDS 44-1418). CF/CoNi is coated by particles such as CoO (JCPDS 75-0533), Co (JCPDS 15-0806), and Ni_3S_2 (JCPDS 30-0863). The particles of these coatings, most of which are nonmagnetic particles, also include magnetic particles. Therefore, we can consider that the magnetic particles coated on the CF/FeCoNi surface are of different types and contents compared to other samples.

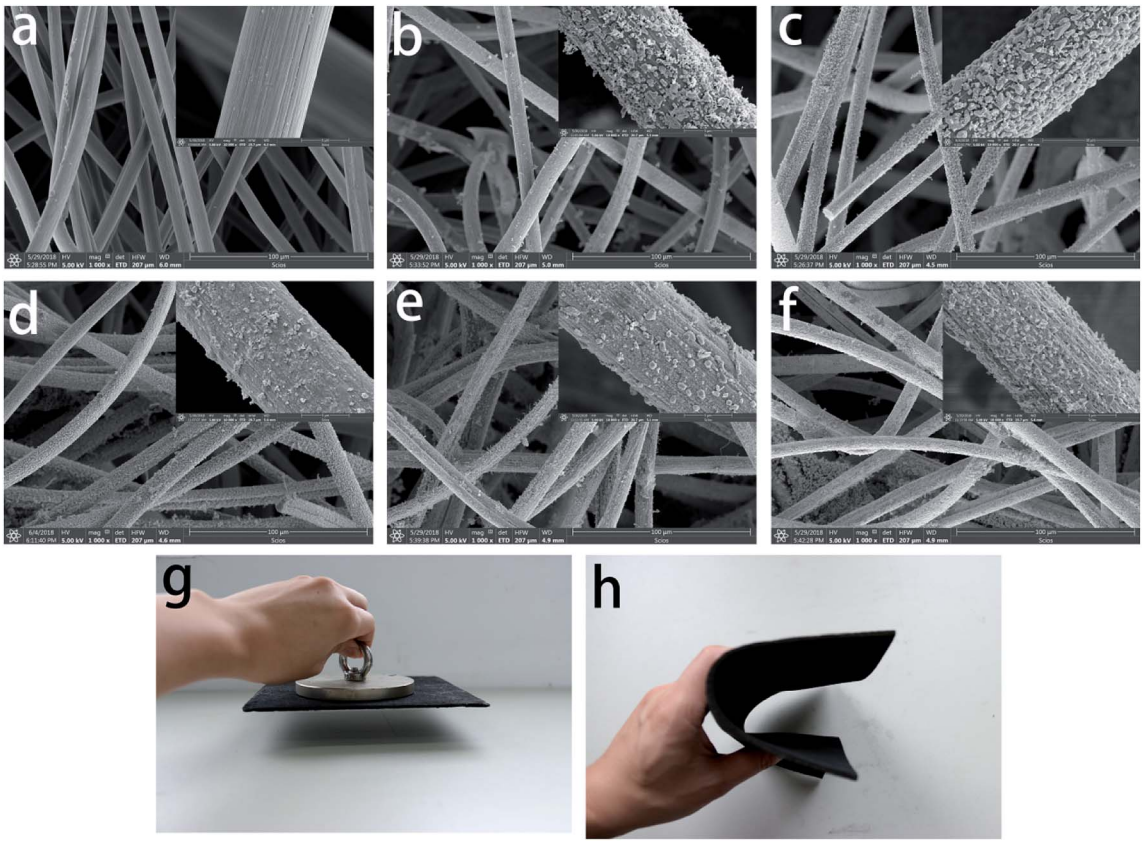

Fig. 3 SEM images of CF/FeCoNi prepared at (a) 0, (b) 0.5, (c) 1, (d) 1.5, (e) 2, and (f) 2.5 times concentration; (g) magnetic and (h) bending properties of CF/FeCoNi prepared at 1 times concentration.

The surface morphology of CF/FeCoNi will also be different when the concentration of the impregnation solution changes. We can see in Fig. 3 that when the concentration of the impregnation solution increases, the number of particles contained in the prepared samples increases. Fig. 3a shows that the surface of the CF (the concentration is 0 times) is smooth and there is no particle coated. When the concentration is 0.5 times (Fig. 3b), there is a certain gap between the particles on the surface of the fiber. When the concentration is greater than 1 times, the magnified image (Fig. 3d–f) reveals a typical plate-like coating; the particle coating on the fiber surface is uniform and tight, and with the increase in concentration, the number of larger particles on the surface of the carbon fiber increases gradually. The increase in the magnetic particle content on the surface of the fiber will affect the electromagnetic wave absorption property of the material.[15] Further, many gaps can be seen between the fibers in the fiber felt, which helps the incident wave to enter the material; the incident wave is reflected in the material many times and produces loss, and there is the improvement in the absorbing property of the material. Fig. 3g shows that CF/FeCoNi (1 times) can be attracted by magnets, which further demonstrates that the fiber surface contains many magnetic particles. In addition, as shown in Fig. 3h, CF/FeCoNi can be bent, which indicates that the material has certain flexibility.

Fig. 4 shows the surface topographic map of CF/FeCo, CF/FeNi, and CF/CoNi obtained from the PAN-based pre-oxidized felt after immersion in the solution with only two salts. We can find that although the concentration of metal ions in the impregnated solution is the same, the distribution of the particles on the surface of the fiber is different, and the particles exhibit a larger aggregation trend, which leads to the larger gap between the particles on the surface of the fiber. It is more obvious that the particles in CF/CoNi are massive, and cannot be uniformly loaded onto the fiber surface. When the impregnated solution contains three metal elements ($FeCl_3$, $CoSO_4 \cdot 7H_2O$, and $NiSO_4 \cdot 6H_2O$), they can form more uniform particles on the fiber surface. The reasons can be further studied.

The EDS spectra of CF, CF/FeCo, CF/FeNi, and CF/CoNi (Fig. 3a, 4a–c) are shown in Fig. 5. Upon immersion in the metal salt solution and treatment at high temperature, there are corresponding C, N, O, S, Cl, Fe, Co, Ni, and other elements on the surface of the fiber. The results show that the surface of the PAN-based pre-oxidative fibers can adsorb metal salts that dissolve in the solution; metal salts undergo thermal degradation after high-temperature treatment and form new particles on the surface of the fibers. Fig. 2 and 3 show that the surface of the CF/FeCoNi fiber contains magnetic particles such as Fe_3O_4, $NiFe_2O_4$, $CoFe_2O_4$, and Ni_3Fe, and their distribution on the surface of the fiber. We can see the EDS surface scan in Fig. 6(c–e); the Fe, Co, and Ni atoms are uniformly dispersed in the fiber on the surface, and the distribution maps are almost overlapped, which proves that the three metal

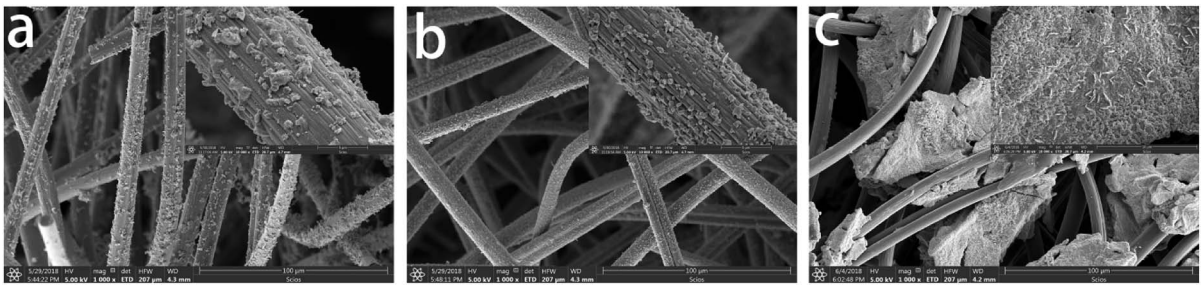

Fig. 4 SEM images of (a) CF/FeCo, (b) CF/FeNi, and (c) CF/CoNi.

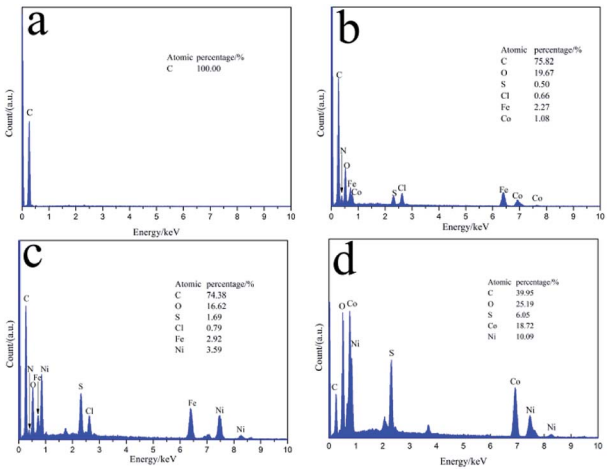

Fig. 5 EDS spectra of (a) CF, (b) CF/FeCo, (c) CF/FeNi, and (d) CF/CoNi.

elements are combined after a series of reactions to generate the magnetic particles; this also agrees with the XRD (Fig. 2a) results.

Formation mechanisms of CF/magnetic particle composite

To analyze the reactions involved in carbonization and understand the formation mechanism of the CF/magnetic particle composite, TG/DSC analyses were performed. Fig. 7 displays the TG curves of pristine CF, and PAN-based pre-oxidized/$FeCl_3$/$CoSO_4\cdot 7H_2O$/$NiSO_4\cdot 6H_2O$ (PAN/metal salt) at a heating rate of 5 °C min^{-1}. There is a proportional weight loss below 100 °C in the TG curves, which is mainly due to the evaporation of moisture. The TG analysis of pristine CF shows one obvious weight loss at 418 °C, which is mainly ascribed to the fast degradation of the PAN-based pre-oxidized fiber, and Fig. 7b shows five weight losses at 138, 380, 505, 607, and 775 °C, which are attributed to the release of crystal water and the degradation of fiber and melt salt ($FeCl_3$, $CoSO_4\cdot 7H_2O$, and $NiSO_4\cdot 6H_2O$), respectively.

However, during the carbonization of PAN/metal salt, the position of the above weight loss peaks slightly changes (see the differential thermal gravimetry (DTG) part of the TG curve), which indicates that the degradation process of PAN-based pre-oxidized fiber and metal salt varies with the interaction between them in the composite fibers.[20] It has been reported that the heating of transition metal salts in an inert atmosphere (namely CO and H_2) leads to an abnormal decomposition.[21,22] This further illustrates a series of reactions such as thermal decomposition and thermal reduction of $FeCl_3$, $CoSO_4\cdot 7H_2O$, and $NiSO_4\cdot 6H_2O$ in the presence of C and at certain temperatures (main reaction processes, such as (1)–(10)). The existence of a series of magnetic particles, such as Fe–Ni, Fe_3O_4, Fe–Co–O, and Fe–Ni–O, and the formation of Fe–Co–Ni, Fe–Co, *etc.* may not reflect the corresponding characteristic peaks in the XRD because of the existence of the amorphous state. The possibility of magnetic particle formation is further confirmed.

$$CoSO_4\cdot 7H_2O \xrightarrow{\Delta,N_2} Co(OH)_2 + H_2O\uparrow + SO_x\uparrow \quad (1)$$

$$NiSO_4\cdot 6H_2O \xrightarrow{\Delta,N_2} Ni(OH)_2 + H_2O\uparrow + SO_x\uparrow \quad (2)$$

$$FeCl_3 + 3H_2O \xrightarrow{\Delta,N_2} Fe(OH)_3 + 3HCl\uparrow \quad (3)$$

$$PAN \xrightarrow{\Delta,N_2} C + CO\uparrow \quad (4)$$

$$Fe(OH)_3 \xrightarrow{\Delta,N_2} Fe_2O_3 + H_2O\uparrow \quad (5)$$

$$Co(OH)_3 \xrightarrow{\Delta,N_2} CoO + H_2O\uparrow \quad (6)$$

$$Ni(OH)_3 \xrightarrow{\Delta,N_2} NiO + H_2O\uparrow \quad (7)$$

$$Fe_2O_3 + CO \text{ or } C \xrightarrow{\Delta,N_2} Fe_3O_4 + CO_2\uparrow \quad (8)$$

$$Fe_2O_3 + CoO + NiO + CO \text{ or } C \xrightarrow{\Delta,N_2} Fe_xCo_yO_z + Fe_xNi_yO_z + CO_2\uparrow \quad (9)$$

$$Fe_xNi_yO_z + CO \text{ or } C \xrightarrow{\Delta,N_2} Fe_xNi_y + CO_2\uparrow \quad (10)$$

Electromagnetic wave absorption properties

Fig. 8 shows the RC of CF and CF/FeCoNi, as a function of frequency, by the NRL-arc method. It shows the influence of concentration on wave absorption; the electromagnetic loss of CF/FeCoNi prepared at low concentration is excellent. It can be seen that the RC of the CF at 5.85–26 GHz was >−2 dB. After coating with magnetic particles, the RC at 5.85–26 GHz was

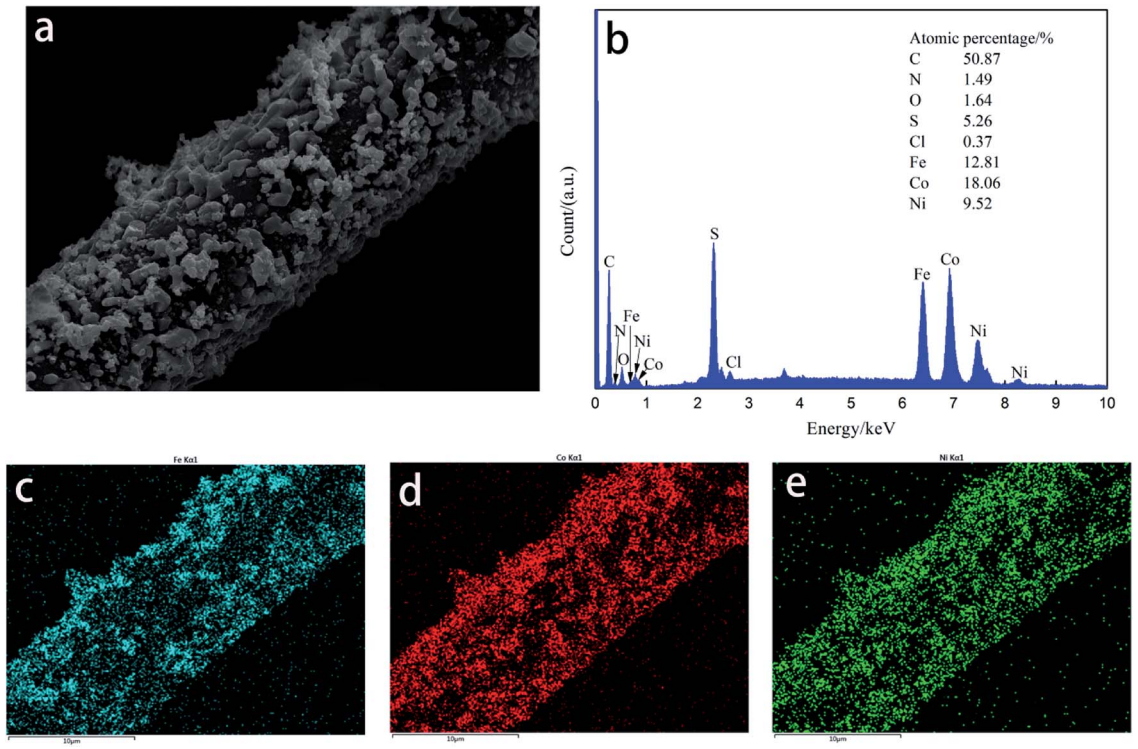

Fig. 6 SEM map scanning topography of CF/FeCoNi neutron absorber composites.

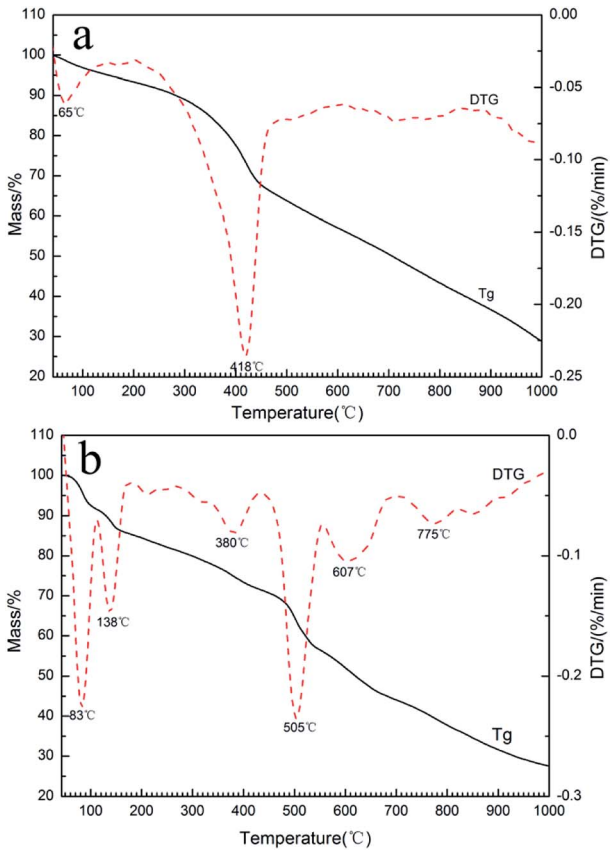

Fig. 7 TG and DTG curves of PAN-based pre-oxidized fiber and PAN/metal salt.

greatly reduced. Magnetic particles, being magnetic loss materials, play a key role in the absorption of electromagnetic waves, and are synergistic with the dielectric loss of carbon fibers, showing excellent wave absorbing properties.[4] When the concentration is 0.5 (0.3125 mol L^{-1}), the RC is <−10 dB (90% of the attenuation), and could reach up to 12.2 GHz (from 13.8 to 26 GHz) (Fig. 8). When the concentration is 1 (0.625 mol L^{-1}), the RC is <−10 dB, and could reach up to 7.4 GHz (from 8.7 to 16.1 GHz), and realizes a minimal RC of −30.62 dB at 15.38 GHz, and an RC better than low concentration (0.5 times) from 5.85 to 15.12 GHz is found. With the increase in the concentration of the solution, the wave absorption of the sample is affected by the concentration of the solution. When the concentration of the impregnated solution is greater than 1 times, the RC of CF/FeCoNi from 5.85 to 26 GHz is >−10 dB. This can be explained as the magnetic particle load of the CF surface being able to increase the electromagnetic wave loss,[12–14] but as the concentration increases, the density of the magnetic particles on the surface of the carbon fiber increases, and the particle size also increases gradually (Fig. 3). All these factors will affect the synergistic effect between the CF (dielectric loss material) and magnetic particles, resulting in wave-absorbing properties, the mechanism of which warrants further study. The NRL-arc method has multiple bell mouths corresponding to different band frequencies; therefore, there is a certain error in the data at the band junction.

The presence of iron, cobalt, and nickel can affect the microwave absorbing properties of the sample (Fig. 9). When $n(\mathrm{Fe}) : n(\mathrm{Co}) : n(\mathrm{Ni}) = 2 : 2 : 1$ (0.625 mol L^{-1}), the RC of the

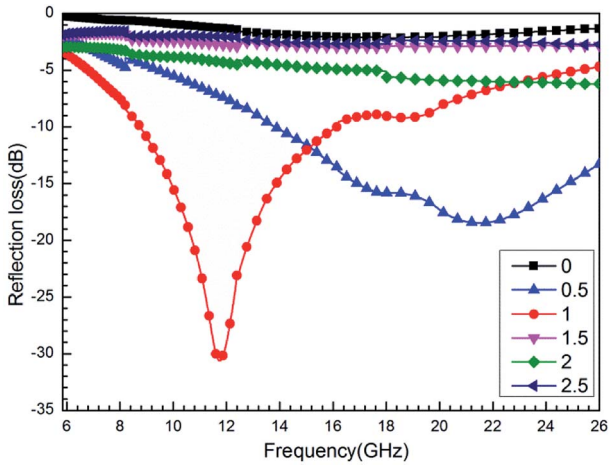

Fig. 8 Reflection loss curves of CF/FeCoNi prepared at 0, 0.5, 1, 1.5, 2, and 2.5 times concentrations.

sample from 5.85 to 16.41 GHz is better than that of the other; it has a minimum RC of −30.62 dB at 11.74 GHz, whereas the effective bandwidth of RC <−10 dB can reach up to 7.4 GHz (from 8.7 to 16.1 GHz). When the frequency band is higher than 16.41 GHz, the RC of CF/FeCo and CF/FeNi is better; this is attributed to the type of particles on the surface of the sample being different. Different magnetic materials show different magnetic loss performance. When the carbon fiber is combined with the dielectric loss material, different wave absorption properties manifest different wavelengths.[23–27] We also found that the addition of Fe could make the CF/magnetic particle composite exhibit better microwave absorption. Through XRD and SEM analysis, we found that the addition of Fe compounds produced more magnetic particles (Fig. 2a) and promoted the uniform distribution of the particles on the surface of the fiber (Fig. 4), Therefore, the RCs of the samples were enhanced. In addition, although the magnetic particles are not found in the CF/CoNi sample, the particles coated on the CF improve the reflection properties of the electromagnetic waves on the surface of the CF, and make the wave-absorbing performance better than that of the CF.[10]

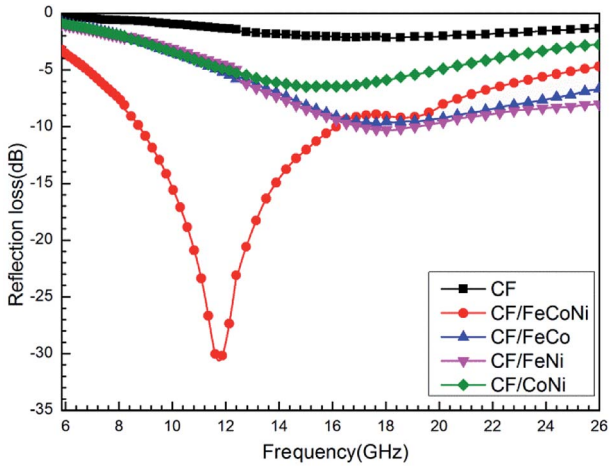

Fig. 9 Reflection loss curves of CF, CF/FeCoNi, CF/FeCo, CF/FeNi, and CF/CoNi.

Conclusions

In summary, a CF/magnetic particle composite was successfully synthesized by the carbonization of an as-impregnated PAN-based pre-oxidized fiber/metal salt, in which the formed magnetic particle can be well dispersed on the surface of CFs. Unlike pristine carbon material, the CF/magnetic particle composite can retain the soft fiber felt structure after carbonization under nitrogen atmosphere. The composites exhibit excellent electromagnetic wave absorption capabilities and wide absorption bandwidths at a lower concentration (0.0625 mol L^{-1}, n(Fe) : n(Co) : n(Ni) = 2 : 2 : 1). The minimum RC of the composite containing the CF/magnetic particle composite can reach up to −30.62 dB at 11.74 GHz due to the enhanced dielectric loss from the magnetic Fe_3O_4, $NiFe_2O_4$, $CoFe_2O_4$, and Ni_3Fe particles and lightweight carbon-based fibers. Moreover, an effective bandwidth (RC below −10 dB) of 7.4 GHz can be achieved in a wide frequency range from 8.7 to 16.1 GHz. These results indicate that the preparation of light soft core (carbon fibers)–shell (magnetic particle) hybrid materials *via* a high-temperature one-step molding process can be considered a promising technique to obtain strong and lightweight electromagnetic wave-absorbing materials in a wide frequency range.

Conflicts of interest

There are no conflicts to declare.

Acknowledgements

This study was supported by the National Key Research and Development Program of China (2016YFB0303100), and the National Science Foundation for Young Scientists of China (Grant No. 51503105).

Notes and references

1 H. Zhu, P. Chen, R. Wu, *et al.*, Microwave absorption properties of carbon fibre containing nonwovens, *Indian J. Fibre Text. Res.*, 2007, **32**, 391–398.
2 B. Wen, X. X. Wang, W. Q. Cao, *et al.*, Reduced graphene oxides: the thinnest and most lightweight materials with highly efficient microwave attenuation performances of the carbon world, *Nanoscale*, 2014, **6**(11), 5754–5761.
3 H. Sun, R. Che, X. You, *et al.*, Crossstacking aligned carbon-nanotube films to tune microwave absorption frequencies and increase absorption intensities, *Adv. Mater.*, 2014, **26**(48), 8120–8125.
4 Y. Qing, D. Min, Y. Zhou, *et al.*, Graphene nanosheet - and flake carbonyl iron particle-filled epoxy–silicone composites as thin–thickness and wide-bandwidth microwave absorber, *Carbon*, 2015, **86**, 98–107.

5 Y. Qing, W. Zhou, F. Luo, *et al.*, Epoxy-silicone filled with multi-walled carbon nanotubes and carbonyl iron particles as a microwave absorber, *Carbon*, 2010, **48**(14), 4074–4080.

6 S. Xia, B. Yao, Q. Chen, *et al.*, Composites with Koch fractal activated carbon fiber felt screens for strong microwave absorption, *Composites, Part B*, 2016, **105**, 1–7.

7 B. Cheng, J. Wang, F. Zhang, *et al.*, Preparation of silver/carbon fiber/polyaniline microwave absorption composite and its application in epoxy resin, *Polym. Bull.*, 2017, **28**, 1–13.

8 Liu, R. Tao, P. Luo, *et al.*, Preparation and microwave absorbing property of carbon fiber/polyurethane radar absorbing coating, *RSC Adv.*, 2017, **7**(73), 46060–46068.

9 M. Arjmand, *Electrical conductivity, electromagnetic interference shielding and dielectric properties of multi-walled carbon nanotube polymer composites*, University of Calgary, 2014.

10 J. Qiu and T. Qiu, Fabrication and microwave absorption properties of magnetite nanoparticle-carbon nanotube-hollow carbon fiber composites, *Carbon*, 2015, **81**(1), 20–28.

11 Y. C. Qing, W. C. Zhou, S. Jia, *et al.*, Electromagnetic and microwave absorption properties of carbonyl iron and carbon fiber filled epoxy/silicone resin coatings, *Appl. Phys. A: Mater. Sci. Process.*, 2010, **100**(4), 1177–1181.

12 X. Chen, X. Wang, L. Li, *et al.*, Preparation and microwave absorbing properties of nickel-coated carbon fiber with polyaniline *via in situ* polymerization, *J. Mater. Sci.: Mater. Electron.*, 2016, **27**(6), 5607–5612.

13 Z. Zeyang, L. Xiangxuan, Z. Haifeng, *et al.*, Electromagnetic and microwave absorption properties of carbon fibers coated with carbonyl iron, *J. Mater. Sci.: Mater. Electron.*, 2015, **26**(9), 6518e25.

14 M. Choi, S. Lee and J. Kim, Clustering effect on the frequency-dependent magnetic properties of Fe-Co micro hollow fiber composites, *IEEE Trans. Magn.*, 2017, 1.

15 Y. Wan, J. Xiao, C. Li, *et al.*, Microwave absorption properties of FeCo-coated carbon fibers with varying morphologies, *J. Magn. Magn. Mater.*, 2016, **399**, 252–259.

16 X. Huang, J. Zhang, W. Rao, *et al.*, Tunable electromagnetic properties and enhanced microwave absorption ability of flaky graphite/cobalt zinc ferrite composites, *J. Alloys Compd.*, 2016, **662**, 409–414.

17 Y. Rao, W. Chen and Z. Cao, Synthesis and Microwave Absorbing Properties of FeCoNi Alloy Particles/Graphite Flaky Composites, *J. Inorg. Mater.*, 2010, **25**(4), 406–410.

18 M. Ning, J. Li, B. Kuang, *et al.*, One-Step Fabrication of N-doped CNTs Encapsulating M nanoparticles (M = Fe, Co, Ni) for Efficient Microwave Absorption, *Appl. Surf. Sci.*, 2018, **447**(31), 244–253.

19 Z. Zhou, C. Lai, L. Zhang, *et al.*, Development of carbon nanofibers from aligned electrospun polyacrylonitrile nanofiber bundles and characterization of their microstructural, electrical, and mechanical properties, *Polymer*, 2009, **50**(13), 2999–3006.

20 C. Sun, Y. Guo, X. Xu, *et al.*, *In situ* preparation of carbon/Fe_3C composite nanofibers with excellent electromagnetic wave absorption properties, *Composites, Part A*, 2017, **92**, 33–41.

21 T. Wanjun and C. Donghua, Mechanism of thermal decomposition of cobalt acetate tetrahydrate, *Chem. Pap.*, 2007, **61**(4), 329–332.

22 J. C. De Jesus, I. González, A. Quevedo, *et al.*, Thermal decomposition of nickel acetate tetrahydrate: an integrated study by TGA, QMS and XPS techniques, *J. Mol. Catal. A: Chem.*, 2005, **228**(1), 283–291.

23 K. Osouli-Bostanabad, H. Aghajani, E. Hosseinzade, H. Maleki-Ghaleh, *et al.*, Microwave Absorption of Nano-Fe_3O_4 Deposited Electrophoretically on Carbon Fiber, *Mater. Manuf. Processes*, 2015, **31**(10), 1351–1356.

24 W. Gan, L. Gao, W. Zhang, *et al.*, Fabrication of microwave absorbing $CoFe_2O_4$ coatings with robust superhydrophobicity on natural wood surfaces, *Ceram. Int.*, 2016, **42**(11), 13199–13206.

25 H. Hosseini and H. Mahdavi, Nanocomposite based on epoxy and MWCNTs modified with $NiFe_2O_4$ nanoparticles as efficient microwave absorbing material, *Appl. Organomet. Chem.*, 2018, **32**(4), e4294.

26 L. I. U. Min, X. I. A. N. G. Jun, W. U. Zhi-Peng, *et al.*, Facile Preparation and Microwave Absorption Properties of Fe-Co-Ni Alloy Nanoparticle Embedded-Carbon Nanofibers, *Chin. J. Inorg. Chem.*, 2017, **1**, 57–65.

27 J. Shim, J. Kim, S. H. Han, *et al.*, Nanocrystalline Fe–Co–Ni–B thin film with high permeability and high-frequency characteristics, *J. Magn. Magn. Mater.*, 2005, **290–291**(s290–291), 205–208.

